Power Allocation for OFDM Wireless Network Localization Under Expectation and Robustness Constraints

Arash Shahmansoori, Gonzalo Seco-Granados, *Senior Member, IEEE*, and Henk Wymeersch, *Member, IEEE*

***Abstract*— In location-aware wireless networks, mobile nodes (agents) can obtain their positions using range measurements to other nodes with known positions (anchors). Optimal subcarrier power allocation at the anchors reduces positioning error and improves network lifetime and throughput. We present an optimization framework for subcarrier power allocations in network localization with the imperfect knowledge of network parameters based on the fundamental statistical limits. Power allocations with expectation and robustness constraints are obtained using semidefinite optimization problems in non-iterative and iterative forms with both unicast and multicast transmissions. Results show that the allocations provide more accurate localization than non-robust designs under channel and agents positions uncertainty.**

***Index Terms*— Wireless network localization, positioning, subcarrier power allocation, OFDM, channel and position uncertainty, robust design, semidefinite optimization, unicast and multicast transmissions.**

I. Introduction

HIGH-ACCURACY localization is of critical importance in many location-based applications and services, e.g., cellular positioning, search-and-rescue tasks, blue-force tracking, communication, and military systems [2], [3]. Wireless network localization (WNL) refers to the process of finding the positions of users (agents) using measurements to nodes with known positions (anchors). The transmission power of the nodes plays an important role in WNL, not only in terms of lifetime and throughput, but also in positioning accuracy [4]. Therefore, an optimal power allocation among both anchors and subcarriers is important for reducing power consumption and increasing positioning accuracy.

Several power allocation methods have been presented for single-carrier transmission in synchronous networks [5], [6]. These methods include the positioning accuracy as either an objective or a constraint, using fundamental performance limits. In [6] and [7] the fundamental limits of wideband localization have been derived in terms of squared position error bound (SPEB) and directional position error bound (DPEB) for the case of single-carrier signals. To overcome the uncertainties on the network parameters, a robust power allocation has been proposed in [9] by converting the minimization of the SPEB and of the maximum DPEB (mDPEB) subject to a total power constraint into semidefinite programming (SDP) and second-order cone programming (SOCP) forms. Meshkati [4], Shen [5], and Shen [8] assumed a unicast transmission scheme, that is to say, when an anchor transmits a signal, it is only listened by one agent. However, for a synchronous network, this leads to suboptimal solutions in terms of total required power by the anchors. Moreover, current and emerging communications standards generally employ multi-carrier signals, in particular orthogonal frequency division multiplexing (OFDM). Multi-carrier transmissions are beneficial when the data rates increase and hence wider bandwidths are needed. Current research for localization using OFDM signals is mainly focused on time delay estimation [10]. In [1], a power allocation for OFDM WNL is developed by converting the optimization into SDP form and numerical averaging over the position error bound.

In this paper, we extend [1] and formulate the power allocations with expectation and robustness constraints in an OFDM WNL with uncertainties on the network parameters (which include the channel coefficients and the positions of the agents) based on the fundamental statistical limits, rather than focusing on a specific localization technique. Our main contributions are:

- We develop a power allocation that minimizes the total power subject to a maximum acceptable value for the expected SPEB, averaged over a set of channel coefficients and agents' positions.
- We develop a power allocation to minimize the total power subject to a maximum acceptable value for the worst-case SPEB, maximized over a set of channel coefficients and agents' positions.

An algorithm is proposed for the case of robust power allocation based on a minimax game and compared with a cutting set method (CSM) [11], while for the power allocation with

Manuscript received May 9, 2016; revised September 8, 2016 and January 20, 2017; accepted January 25, 2017. Date of current version March 8, 2017. This work was supported in part by the EU FP7 Marie Curie Initial Training Network Multi-Technology Positioning Professionals (MULTIPOS) under Grant 316528, in part by the European Research Council under Grant 258418 (COOPNET), in part by the Horizon2020 Project High Precision Positioning for Cooperative ITS Applications (HIGHTS) under Grant MG-3.5a-2014-636537, and in part by the R&D Project of Spanish Ministry of Economy and Competitiveness under Grant TEC2014-53656-R. Part of this paper was presented at the 2015 IEEE International Conference on Communication Workshop [1]. The associate editor coordinating the review of this paper and approving it for publication was A. Giorgetti.

A. Shahmansoori and G. Seco-Granados are with the Department of Telecommunications and Systems Engineering, Universitat Autònoma de Barcelona, 08193 Barcelona, Spain (e-mail: arash.shahmansoori@uab.cat; gonzalo.seco@uab.cat).

H. Wymeersch is with the Department of Signals and Systems, Chalmers University of Technology, 41296 Göteborg, Sweden (e-mail: henkw@chalmers.se).

Color versions of one or more of the figures in this paper are available online at http://ieeexplore.ieee.org.

Digital Object Identifier 10.1109/TWC.2017.2662678

expectation constraints, we propose the use of the sample average as an approximation of the expectation. Both methods are approximate, but turn out to perform well under the considered scenarios. In particular, the convergence of the robust power allocation is not shown analytically but only demonstrated empirically by simulations in a reasonable setting for a specific set of parameters.

The remainder of this paper is organized as follows. The system model, including the different types of uncertainty, are presented in Section II. A standard non-robust power allocation, ignoring uncertainty, is summarized in Section III. The proposed power allocations with expectation and robustness constraints are derived in Sections IV and V, respectively. The different approaches are compared numerically in Section VI, before we draw conclusions in Section VII.

Notation: $\mathrm{diag}\{\mathbf{X}_m\}_{m\in\mathcal{M}}$ denotes the block-diagonal matrix with the mth block equal to $\mathbf{X}_m$ and m in the set of indices $\mathcal{M}$; $\mathrm{diag}\{x_m\}_{m=0}^{M-1}$ denotes an $M \times M$ diagonal matrix formed with the values x_m; $\{\mathbf{x}_i\}$ represents the set of all vectors $\mathbf{x}_i$ for all possible values of the subindex i; $\mathbf{I}_N$ is the $N \times N$ identity matrix; $\mathbf{1}_N$ is the $N\times 1$ all-one vector; $\|.\|$ denotes the l_2-norm; $\otimes$ denotes the Kronecker product; $\mathrm{tr}\{\mathbf{X}\}$ denotes the trace of the matrix $\mathbf{X}$; $\mathbf{X} \succeq \mathbf{Y}$ means that the matrix $\mathbf{X}-\mathbf{Y}$ is positive semi-definite (PSD); $\mathbf{X} \succ \mathbf{Y}$ means that the matrix $\mathbf{X}-\mathbf{Y}$ is positive definite; $\mathbf{x} \succeq \mathbf{y}$ and $\mathbf{x} \succ \mathbf{y}$ mean that all the elements of $\mathbf{x}-\mathbf{y}$ are nonnegative and positive, respectively; and $\Re\{.\}$ and $\Im\{.\}$ denote the real and imaginary parts, respectively.

II. System Model

In this section, we present the signal model for multi-carrier network localization. Then, uncertainty models for network parameters are defined.

A. Observation Model

Consider a wireless network with N_b anchors with known positions and N_a agents with unknown positions. The sets of agents and anchors are denoted by $\mathcal{N}_a = \{1,\ldots,N_a\}$ and $\mathcal{N}_b = \{N_a+1,\ldots,N_a+N_b\}$, respectively. The two-dimensional positions of kth agent and jth anchor are denoted by $\mathbf{q}_k = [x_k\ y_k]^{\mathrm{T}}$ for $k \in \mathcal{N}_a$ and $\mathbf{q}_j = [x_j\ y_j]^{\mathrm{T}}$ for $j \in \mathcal{N}_b$. Anchors may be elements of the fixed infrastructure, whereas agents may be mobile users. We assume that all nodes are perfectly synchronized [9] and use OFDM transmissions from anchors to agents to localize the agents. We will focus on the case where each anchor j sends an OFDM signal, which is received by *all* agents (multicast transmission). However, all methods are easily modified for the case where each anchor j sends an OFDM signal that is received by *one* agent at a time (unicast transmission).

We denote as $\mathbf{r}_{k,j}$ the $N\times 1$ vector representing the received signal by agent k produced by the transmission of anchor j with N subcarriers, after cyclic prefix removal and transformation to the frequency domain. The vector $\mathbf{r}_{k,j}$ can be expressed as [12]–[14]

$$\mathbf{r}_{k,j} = \Gamma(t_{k,j})\mathbf{B}_j\mathbf{F}_L\mathbf{h}_{k,j} + \mathbf{w}_{k,j}, \tag{1}$$

where $\mathbf{B}_j = \mathrm{diag}\{B_j[n]\}_{n=-N/2}^{N/2}$ is an $N\times N$ diagonal matrix representing the N symbols sent by anchor j on each of the subcarriers, $\mathbf{F}_L$ represents the first L columns of the $N\times N$ discrete Fourier transform (DFT) matrix with L being the number of channel taps between nodes j and k (without loss of generality, we assume the same number of taps for all channels), $\mathbf{h}_{k,j} = [h_{k,j}^{(1)} \ldots h_{k,j}^{(L)}]^{\mathrm{T}}$ with the real and imaginary parts defined as $\mathbf{h}_{R,k,j}$ and $\mathbf{h}_{I,k,j}$ is the channel response between the corresponding anchor and agent, respectively, $\Gamma(t_{k,j}) = \mathrm{diag}\{\exp(-j2\pi n t_{k,j}/T)\}_{n=-N/2}^{N/2}$ where $t_{k,j}$ is the arrival time of the first path and is given by $t_{k,j} = \|\mathbf{q}_k - \mathbf{q}_j\|/c$ with c representing the speed of light. The symbol time duration is denoted as T, and $\mathbf{w}_{k,j}$ is an $N\times 1$ noise vector distributed as $\mathcal{CN}(\mathbf{0},\sigma_w^2\mathbf{I}_N)$. We introduce $\mathbf{r}$ as the vector representation of the received waveforms by all agents from all anchors, given by $\mathbf{r} = [\mathbf{r}_1^{\mathrm{T}}\ \ldots\ \mathbf{r}_{N_a}^{\mathrm{T}}]^{\mathrm{T}}$ with $\mathbf{r}_k = [\mathbf{r}_{k,N_a+1}^{\mathrm{T}}\ \ldots\ \mathbf{r}_{k,N_a+N_b}^{\mathrm{T}}]^{\mathrm{T}}$.

Note that for unicast operation, each anchor j will send different OFDM signals to each agent. In terms of the model, the only difference is that we have to replace $\mathbf{B}_j$ by $\mathbf{B}_{k,j}$ in (1).

Our goal is to minimize the total transmission power ($P_{\mathrm{T,multi}} = \sum_{j\in\mathcal{N}_b}\mathrm{tr}\{\mathbf{P}_j\}$ where $\mathbf{P}_j = \mathbf{B}_j^{\mathrm{H}}\mathbf{B}_j$ for multicast and $P_{\mathrm{T,uni}} = \sum_{k\in\mathcal{N}_a}\sum_{j\in\mathcal{N}_b}\mathrm{tr}\{\mathbf{P}_{k,j}\}$ where $\mathbf{P}_{k,j} = \mathbf{B}_{k,j}^{\mathrm{H}}\mathbf{B}_{k,j}$ for unicast) required to obtain a certain positioning accuracy in terms of the fundamental statistical limits in the presence of uncertainties in the channel and the agent positions. We note that we do not consider different sets of subcarriers for different users, so that each user can make use of the full system bandwidth.

B. Uncertainty Model

We consider a scenario in which we have some a priori information regarding the channel coefficients and the locations of the agents.

For the channel, we consider that $\mathbf{h}_{k,j} = \hat{\mathbf{h}}_{k,j} + \Delta\mathbf{h}_{k,j}$, where $\hat{\mathbf{h}}_{k,j}$ is an a priori estimate of the channel and $\Delta\mathbf{h}_{k,j}$ is the uncertainty on the channel, belonging to either the sets $\mathcal{H}_{k,j}^{(1)}$ or $\mathcal{H}_{k,j}^{(2)}$, with

$$\mathcal{H}_{k,j}^{(1)} \triangleq \left\{\Delta\mathbf{h}_{k,j} : \|\Delta\mathbf{h}_{k,j}\| \le \epsilon\right\}, \tag{2}$$

$$\mathcal{H}_{k,j}^{(2)} \triangleq \left\{\Delta\mathbf{h}_{k,j} : |\Delta h_{k,j,l}| \le \epsilon_l, l = 1,\ldots,L\right\}. \tag{3}$$

Here, $\Delta h_{k,j,l}$ is the uncertainty of the lth channel tap, while ϵ_l and ϵ represent bounds on the uncertainty. Denoting by $\phi_{k,j} = \pm\arctan(y_k - y_j)/(x_k - x_j)$ the angle between the jth anchor and kth agent with respect to the positive x axis (with positive sign for $x_k > x_j$ and $y_k > y_j$ or $x_k < x_j$ and $y_k < y_j$ and negative sign otherwise), we can write $\phi_{k,j} = \hat{\phi}_{k,j} + \Delta\phi_{k,j}$, where $\hat{\phi}_{k,j}$ is an a priori estimate and $\Delta\phi_{k,j}$ is the uncertainty of the angle, limited to $|\Delta\phi_{k,j}| \le \delta_{k,j}$, with $0 \le \delta_{k,j} < \pi/2$. Fig. 1 shows the network scheme with four anchors and the k-th agent with the agent's actual position to lie within a circle of radius ϵ_d, and the relative angle between the kth agent and the jth anchor is shown by $\phi_{k,j}$.

III. Non-Robust Power Allocation

In this section, we provide the SPEB for OFDM signals and the formulation of the non-robust power allocation, without considering any uncertainties.

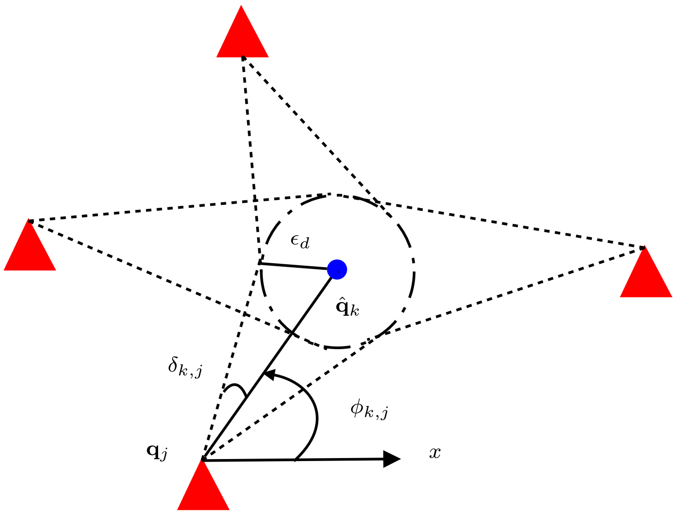

Fig. 1. Illustration of the uncertainty model for WNL for agent k with the angular uncertainty $\delta_{k,j}$ and the relative angle $\phi_{k,j}$.

A. Squared Position Error Bound

We consider the agents' positions and channel coefficients as deterministic unknown parameters and we determine the corresponding Fisher information matrix (FIM). From this FIM, we can derive the SPEB. Let us define $\boldsymbol{\eta} = [\mathbf{q}_1^{\mathrm{T}} \dots \mathbf{q}_{N_a}^{\mathrm{T}}\ \boldsymbol{\theta}_1^{\mathrm{T}} \dots \boldsymbol{\theta}_{N_a}^{\mathrm{T}}]^{\mathrm{T}}$ where the whole set of channel coefficients is $\boldsymbol{\theta}_k = [\mathbf{k}_{k,N_a+1}^{\mathrm{T}} \dots \mathbf{k}_{k,N_a+N_b}^{\mathrm{T}}]^{\mathrm{T}}$, in which $\mathbf{k}_{k,j} = [\mathbf{h}_{R,k,j}^{\mathrm{T}}\ \mathbf{h}_{I,k,j}^{\mathrm{T}}]^{\mathrm{T}}$. The FIM of the parameters in $\boldsymbol{\eta}$ is

$$\mathbf{J}_{\boldsymbol{\eta}} = \mathbb{E}_{\mathbf{r}|\boldsymbol{\eta}}[-\frac{\partial^2 \ln f(\mathbf{r};\boldsymbol{\eta})}{\partial\boldsymbol{\eta}\partial\boldsymbol{\eta}^{\mathrm{T}}}]. \tag{4}$$

This FIM is a $2(N_aN_bL + N_a) \times 2(N_aN_bL + N_a)$ real PSD matrix, with the property that for any unbiased estimate $\hat{\boldsymbol{\eta}}$ of $\boldsymbol{\eta}$, it holds that [15]

$$\mathbb{E}_{\mathbf{r}|\boldsymbol{\eta}}[(\hat{\boldsymbol{\eta}} - \boldsymbol{\eta})(\hat{\boldsymbol{\eta}} - \boldsymbol{\eta})^{\mathrm{T}}] \succeq \mathbf{J}_{\boldsymbol{\eta}}^{-1}. \tag{5}$$

The FIM $\mathbf{J}_{\boldsymbol{\eta}}$ has the following form

$$\mathbf{J}_{\boldsymbol{\eta}} = \begin{bmatrix} \Phi(\mathbf{q},\mathbf{q}) & \Phi(\mathbf{q},\boldsymbol{\theta}_1) & \dots & \Phi(\mathbf{q},\boldsymbol{\theta}_{N_a}) \\ \Phi(\boldsymbol{\theta}_1,\mathbf{q}) & \Phi(\boldsymbol{\theta}_1,\boldsymbol{\theta}_1) & \dots & \Phi(\boldsymbol{\theta}_1,\boldsymbol{\theta}_{N_a}) \\ \vdots & & \ddots & \vdots \\ \Phi(\boldsymbol{\theta}_{N_a},\mathbf{q}) & \Phi(\boldsymbol{\theta}_{N_a},\boldsymbol{\theta}_1) & \dots & \Phi(\boldsymbol{\theta}_{N_a},\boldsymbol{\theta}_{N_a}) \end{bmatrix}, \tag{6}$$

where we have used the following definitions $\mathbf{q} = [\mathbf{q}_1^{\mathrm{T}} \dots \mathbf{q}_{N_a}^{\mathrm{T}}]^{\mathrm{T}}$,

$$\Phi(\mathbf{x},\mathbf{y}) \triangleq \frac{2}{\sigma_w^2}\Re\left\{\frac{\partial\boldsymbol{\mu}^{\mathrm{H}}}{\partial\mathbf{x}}\frac{\partial\boldsymbol{\mu}}{\partial\mathbf{y}^{\mathrm{T}}}\right\}, \tag{7}$$

and $\boldsymbol{\mu} \triangleq \bar{\Gamma}(\mathbf{t})(\mathbf{I}_{N_a} \otimes \mathbf{B})\bar{\mathbf{F}}_L\mathbf{h}$ with $\bar{\Gamma}(\mathbf{t}) = \mathrm{diag}\{\bar{\Gamma}(\mathbf{t}_k)\}_{k\in\mathcal{N}_a}$, $\mathbf{B} = \mathrm{diag}\{\mathbf{B}_j\}_{j\in\mathcal{N}_b}$, $\bar{\mathbf{F}}_L = \mathbf{I}_{N_aN_b} \otimes \mathbf{F}_L$, $\mathbf{h} = [\mathbf{h}_1^{\mathrm{T}} \dots \mathbf{h}_{N_a}^{\mathrm{T}}]^{\mathrm{T}}$, in which $\bar{\Gamma}(\mathbf{t}_k)$ and $\mathbf{h}_k$ are defined as $\bar{\Gamma}(\mathbf{t}_k) = \mathrm{diag}\{\Gamma(t_{k,j})\}_{j\in\mathcal{N}_b}$ and $\mathbf{h}_k = [\mathbf{h}_{k,N_a+1}^{\mathrm{T}}\ \dots\ \mathbf{h}_{k,N_a+N_b}^{\mathrm{T}}]^{\mathrm{T}}$. The terms $\Phi(\boldsymbol{\theta}_k,\boldsymbol{\theta}_m)$, $\Phi(\mathbf{q}_k,\mathbf{q}_m)$, $\Phi(\boldsymbol{\theta}_m,\mathbf{q}_k)$, and $\Phi(\mathbf{q}_k,\boldsymbol{\theta}_m)$ are zero for $k \neq m$ (see Appendix A), so that the equivalent FIM (EFIM) of the agents' positions is given by

$$\mathbf{J}_e(\mathbf{q}) = \zeta\sum_{j\in\mathcal{N}_b}\mathrm{diag}\{\lambda_{1,j}\mathbf{J}_r(\phi_{1,j}),\dots,\lambda_{N_a,j}\mathbf{J}_r(\phi_{N_a,j})\}, \tag{8}$$

where $\zeta = 2/(c^2\sigma_w^2)$, $\mathbf{J}_r(\phi_{k,j}) = \mathbf{u}_r(\phi_{k,j})\mathbf{u}_r^{\mathrm{T}}(\phi_{k,j})$ with $\mathbf{u}_r(\phi_{k,j}) = [\cos\phi_{k,j}\ \ \sin\phi_{k,j}]^{\mathrm{T}}$ is the so-called ranging direction matrix (RDM) and $\lambda_{k,j}$ is the ranging information intensity (RII), given by [1]

$$\lambda_{k,j} = \mathbf{h}_{k,j}^{\mathrm{H}}\mathbf{M}_j^{(1)}(\mathbf{p}_j)\mathbf{h}_{k,j} - \mathbf{h}_{k,j}^{\mathrm{H}}\mathbf{M}_j^{(2)}(\mathbf{p}_j)\mathbf{h}_{k,j}, \tag{9}$$

where

$$\mathbf{M}_j^{(1)}(\mathbf{p}_j) = \mathbf{F}_L^{\mathrm{H}}\mathbf{D}^{\mathrm{H}}\mathbf{P}_j\mathbf{D}\mathbf{F}_L, \tag{10}$$

$$\mathbf{M}_j^{(2)}(\mathbf{p}_j) = \Xi^{\mathrm{H}}(\mathbf{p}_j)\Sigma^{-1}(\mathbf{p}_j)\Xi(\mathbf{p}_j), \tag{11}$$

in which $\mathbf{D} = \mathrm{diag}\{j2\pi n/T\}_{n=-N/2}^{N/2}$, $\Xi(\mathbf{p}_j) = \mathbf{F}_L^{\mathrm{H}}\mathbf{P}_j\mathbf{D}\mathbf{F}_L$, and $\Sigma(\mathbf{p}_j) = \mathbf{F}_L^{\mathrm{H}}\mathbf{P}_j\mathbf{F}_L$. Finally, the SPEB for kth agent is given by

$$\mathcal{P}_k(\{\mathbf{p}_j\}) \triangleq \mathrm{tr}\{\mathbf{J}_e^{-1}(\mathbf{q}_k)\}, \tag{12}$$

where $\mathbf{p}_j$ is the $N \times 1$ vector of transmitted power taken from the main diagonal of $\mathbf{P}_j$, and

$$\mathbf{J}_e(\mathbf{q}_k) = \zeta\sum_{j\in\mathcal{N}_b}\lambda_{k,j}\mathbf{J}_r(\phi_{k,j}). \tag{13}$$

B. Formulation of the Non-Robust Power Allocation Problem

The non-robust power allocation consists in obtaining the values of $\{\mathbf{p}_j\}$ that are optimum for the estimated values of the channel and angles, $\hat{\mathbf{h}}_{k,j}$ and $\hat{\phi}_{k,j}$, which are therefore used in the formulation of the problem. For multicast[1] transmission, it has the following form

$$\mathcal{A}_{\mathrm{NR}}:\ \underset{\{\mathbf{p}_j\}}{\mathrm{minimize}}\ \sum_{j\in\mathcal{N}_b}\mathbf{1}^{\mathrm{T}}\mathbf{p}_j \tag{14a}$$

$$\text{subject to } \mathcal{P}_k(\{\mathbf{p}_j\}) \leq \beta,\quad \forall k \in \mathcal{N}_a \tag{14b}$$

$$\mathbf{p}_j \succeq \mathbf{0},\quad \forall j \in \mathcal{N}_b \tag{14c}$$

where β is maximum acceptable SPEB of the agents. We note that: (14a) aims at minimizing the total power of the anchors required to localize the agents; (14b) sets an upper bound β to the SPEB of the agents; (14c) restricts the anchor power vectors $\mathbf{p}_j$ to be non-negative. Problem $\mathcal{A}_{\mathrm{NR}}$ is the extension to multi-carrier signals of minimum energy cost problem in [9] for multicast transmission. Finally, we note that $\mathcal{A}_{\mathrm{NR}}$ is a convex optimization problem.

The problem $\mathcal{A}_{\mathrm{NR}}$ can be written in the SDP form [16] by replacing each constraint in (14b) by

$$\mathbf{J}_e(\mathbf{q}_k) \succeq \widetilde{\mathbf{G}}_k, \tag{15}$$

$$\widetilde{\Theta}(\widetilde{\mathbf{G}}_k;\beta) \succeq \mathbf{0}, \tag{16}$$

where $\widetilde{\mathbf{G}}_k$ is a 2×2 auxiliary matrix and

$$\widetilde{\Theta}(\widetilde{\mathbf{G}}_k;\beta) = \begin{bmatrix} \beta & \widetilde{\mathbf{v}}_1^{\mathrm{T}} & \widetilde{\mathbf{v}}_2^{\mathrm{T}} \\ \widetilde{\mathbf{v}}_1 & \widetilde{\mathbf{G}}_k & \mathbf{0} \\ \widetilde{\mathbf{v}}_2 & \mathbf{0} & \widetilde{\mathbf{G}}_k \end{bmatrix}, \tag{17}$$

where $\widetilde{\mathbf{v}}_1 = [1,0]^{\mathrm{T}}$ and $\widetilde{\mathbf{v}}_2 = [0,1]^{\mathrm{T}}$. Moreover, the matrix inequality $\mathbf{J}_e(\mathbf{q}_k) \succeq \widetilde{\mathbf{G}}_k$ can be written as a linear matrix

[1]All of the optimization problems within this paper can be easily reformulated for unicast transmission by replacing $\mathbf{p}_j$ with $\mathbf{p}_{k,j}$ and $\sum_{j\in\mathcal{N}_b}\mathbf{1}^{\mathrm{T}}\mathbf{p}_j$ with $\sum_{k\in\mathcal{N}_a}\sum_{j\in\mathcal{N}_b}\mathbf{1}^{\mathrm{T}}\mathbf{p}_{k,j}$ with $\mathbf{p}_{k,j}$ defined as an $N \times 1$ power vector for transmission from the jth anchor to the kth agent.

inequality on the power vector $\mathbf{p}_j$. In particular, we can replace $\mathbf{J}_e(\mathbf{q}_k) \succeq \widetilde{\mathbf{G}}_k$ by $\Pi_k(\{\mathbf{p}_j\}, \widetilde{\mathbf{G}}_k) \succeq \mathbf{0}$, where

$$\Pi_k(\{\mathbf{p}_j\}, \widetilde{\mathbf{G}}_k) = \begin{bmatrix} \sum_{j\in\mathcal{N}_b} \nu_{k,j}(\mathbf{p}_j)\mathbf{J}_r(\hat{\phi}_{k,j}) - \widetilde{\mathbf{G}}_k & \Psi_k^{\mathrm{H}}(\{\mathbf{p}_j\}) \\ \Psi_k(\{\mathbf{p}_j\}) & \Sigma(\{\mathbf{p}_j\}) \end{bmatrix}, \quad (18)$$

where $\nu_{k,j}(\mathbf{p}_j) = \zeta \hat{\mathbf{h}}_{k,j}^{\mathrm{H}}\mathbf{M}_j^{(1)}(\mathbf{p}_j)\hat{\mathbf{h}}_{k,j}$, $\Psi_k^{\mathrm{H}}(\{\mathbf{p}_j\}) = [\Psi_{k,1}^{\mathrm{H}}(\mathbf{p}_1)\dots\Psi_{k,N_b}^{\mathrm{H}}(\mathbf{p}_{N_b})]$ and $\Psi_{k,j}^{\mathrm{H}}(\mathbf{p}_j) = \sqrt{\zeta}\mathbf{u}_r(\hat{\phi}_{k,j})\hat{\mathbf{h}}_{k,j}^{\mathrm{H}}\,\Xi^{\mathrm{H}}(\mathbf{p}_j)$, $\Sigma(\{\mathbf{p}_j\}) = \mathrm{diag}\{\Sigma(\mathbf{p}_1),\dots,\Sigma(\mathbf{p}_{N_b})\}$.

The non-robust design uses only the estimated channel coefficients and agent locations for the power allocation problem. The main drawback of the proposed non-robust allocation is that the designed power allocation is specific for particular network parameters. This causes the actual SPEB to deviate from the maximum value β when the agent's real positions and channels do not coincide with the ones used in the design. The goal of the power allocations is to control this deviation by taking into account in the design the uncertainty between the real parameters (i.e., channels and positions) and those assumed for the design.

IV. Power Allocation With Expectation Constraints

In this section, we introduce the power allocation with expectation constraints and convert it to an SDP form. The power allocation problem for the case of multicast design has the following form

$$\mathcal{A}_{\mathrm{E}}: \ \underset{\{\mathbf{p}_j\}}{\text{minimize}} \ \sum_{j\in\mathcal{N}_b} \mathbf{1}^{\mathrm{T}}\mathbf{p}_j \quad (19a)$$

$$\text{subject to } \mathbb{E}_{\boldsymbol{\eta}}[\mathrm{tr}\{\mathbf{J}_e^{-1}(\mathbf{q}_k)\}] \le \beta, \quad \forall k \in \mathcal{N}_a \quad (19b)$$

$$\mathbf{p}_j \succeq \mathbf{0}. \quad \forall j \in \mathcal{N}_b \quad (19c)$$

We note that (19b) sets an upper bound β to the *expected* SPEB of the agents, with respect to the channel coefficients $\mathbf{h}_{k,j}$ and agents' positions $\mathbf{q}_k$. Given that the analytical calculation of (19b) is inaccessible, we resort to a numerical approximation by averaging over M_q realizations:

$$\frac{1}{M_q}\sum_{m=1}^{M_q} \mathrm{tr}\{[\mathbf{J}_{e,k,m}^{-1}(\{\mathbf{p}_j\})]\} \le \beta, \quad (20)$$

where

$$\mathbf{J}_{e,k,m}(\{\mathbf{p}_j\}) = \zeta \sum_{j\in\mathcal{N}_b} \lambda_{k,j,m}\mathbf{J}_r(\phi_{k,j,m}), \quad (21)$$

$$\lambda_{k,j,m} = \mathbf{h}_{k,j,m}^{\mathrm{H}}(\mathbf{M}_j^{(1)}(\mathbf{p}_j) - \mathbf{M}_j^{(2)}(\mathbf{p}_j))\mathbf{h}_{k,j,m}, \quad (22)$$

with $\mathbf{h}_{k,j,m}$ and $\phi_{k,j,m}$ being generated according to one of the uncertainty models in Section II-B.

Using the same approach as in Section III-B, we can reformulate $\mathcal{A}_{\mathrm{E}}$ in SDP form as

$$\mathcal{A}_{\mathrm{E}}^{\mathrm{SDP}}: \ \underset{\{\mathbf{p}_j\},\{\mathbf{G}_k\}}{\text{minimize}} \ \sum_{j\in\mathcal{N}_b} \mathbf{1}^{\mathrm{T}}\mathbf{p}_j \quad (23a)$$

$$\text{subject to } \Theta(\mathbf{G}_k;\beta) \succeq \mathbf{0}, \forall k \in \mathcal{N}_a \quad (23b)$$

$$\Pi_{k,m}(\{\mathbf{p}_j\}, \mathbf{G}_{k,m}) \succeq \mathbf{0}, \quad \forall m \in \mathcal{M}_q \quad (23c)$$

$$\mathbf{p}_j \succeq \mathbf{0}, \quad \forall j \in \mathcal{N}_b \quad (23d)$$

where $\mathcal{M}_q = \{1,\dots,M_q\}$, $\mathbf{G}_k = \mathrm{diag}\{\mathbf{G}_{k,m}\}_{m=1}^{M_q}$ comprises M_q auxiliary 2×2 matrices $\mathbf{G}_{k,m}$,

$$\Theta(\mathbf{G}_k;\beta) = \begin{bmatrix} M_q\beta & \mathbf{v}_1^{\mathrm{T}} & \mathbf{v}_2^{\mathrm{T}} \\ \mathbf{v}_1 & \mathbf{G}_k & \mathbf{0} \\ \mathbf{v}_2 & \mathbf{0} & \mathbf{G}_k \end{bmatrix}, \quad (24)$$

with $\mathbf{v}_1 = \mathbf{1}_{M_q} \otimes \widetilde{\mathbf{v}}_1$ and $\mathbf{v}_2 = \mathbf{1}_{M_q} \otimes \widetilde{\mathbf{v}}_2$. The matrix $\Pi_{k,m}(\{\mathbf{p}_j\}, \mathbf{G}_{k,m})$ is defined as

$$\Pi_{k,m}(\{\mathbf{p}_j\}, \mathbf{G}_{k,m}) = \begin{bmatrix} \sum_{j\in\mathcal{N}_b} \nu_{k,j,m}(\mathbf{p}_j)\mathbf{J}_r(\phi_{k,j,m}) - \mathbf{G}_{k,m} & \Psi_{k,m}^{\mathrm{H}}(\{\mathbf{p}_j\}) \\ \Psi_{k,m}(\{\mathbf{p}_j\}) & \Sigma(\{\mathbf{p}_j\}) \end{bmatrix}, \quad (25)$$

in which $\nu_{k,j,m}(\mathbf{p}_j) = \zeta \mathbf{h}_{k,j,m}^{\mathrm{H}}\mathbf{M}_j^{(1)}(\mathbf{p}_j)\mathbf{h}_{k,j,m}$, and $\Psi_{k,m}^{\mathrm{H}}(\{\mathbf{p}_j\}) = [\Psi_{k,1,m}^{\mathrm{H}}(\mathbf{p}_1)\dots\Psi_{k,N_b,m}^{\mathrm{H}}(\mathbf{p}_{N_b})]$, with $\Psi_{k,j,m}^{\mathrm{H}}(\mathbf{p}_j) = \sqrt{\zeta}\mathbf{u}_r(\phi_{k,j,m})\mathbf{h}_{k,j,m}^{\mathrm{H}}\,\Xi^{\mathrm{H}}(\mathbf{p}_j)$.

V. Robust Power Allocation

In this section, we propose a robust power allocation, accounting for the worst-case channel and position uncertainty.

A. General Formulation

The robust power allocation problem for multicast design is of the following form

$$\mathcal{A}_{\mathrm{R}}: \ \underset{\{\mathbf{p}_j\}}{\text{minimize}} \ \sum_{j\in\mathcal{N}_b} \mathbf{1}^{\mathrm{T}}\mathbf{p}_j \quad (26a)$$

$$\text{subject to } \mathcal{P}_k^{\max}(\{\mathbf{p}_j\}) \le \beta, \quad \forall k \in \mathcal{N}_a \quad (26b)$$

$$\mathbf{p}_j \succeq \mathbf{0}, \quad \forall j \in \mathcal{N}_b \quad (26c)$$

where $\mathcal{P}_k^{\max}(\{\mathbf{p}_j\})$ is the worst-case SPEB:

$$\mathcal{P}_k^{\max}(\{\mathbf{p}_j\}) \triangleq \max_{\mathbf{h}_k,\boldsymbol{\phi}_k} \mathcal{P}_k(\{\mathbf{p}_j\}), \quad (27)$$

in which $\boldsymbol{\phi}_k = [\phi_{k,N_a+1}\dots\phi_{k,Na+Nb}]^{\mathrm{T}}$. We note that since (27) is the pointwise maximum over convex functions, the problem $\mathcal{A}_{\mathrm{R}}$ is a convex problem. Therefore, there is a variety of algorithms to solve the robust power allocation with guaranteed convergence (e.g., a cutting plane method), but with high complexity. Our ambition is to propose a potentially suboptimal method but with a reduced complexity. We will achieve this by solving the problem through a minimax game, where one player chooses a best power allocation and the second player the worst possible channel. Such an approach does not necessarily converge, unless the constraints satisfy certain technical conditions [16, Sec. 10.3.4]. However, simulations will show that in practice our algorithm performs very similar to the solution obtained using the more complex CSM, which has guaranteed convergence [11].

Due to the structure of the SPEB in (8), the maximization over $\phi_{k,j}$ for any given value of $\mathbf{h}_{k,j}$ can be determined as in [9], by replacing $\mathbf{J}_r(\phi_{k,j})$ with $\mathbf{Q}_r(\hat{\phi}_{k,j},\delta_{k,j}) = \mathbf{J}_r(\hat{\phi}_{k,j}) - \sin\delta_{k,j}\mathbf{I}_2$. Later, we will rely on the eigen-decomposition of $\mathbf{Q}_r(\hat{\phi}_{k,j},\delta_{k,j})$. It is readily verified that the two eigenvectors of $\mathbf{Q}_r(\hat{\phi}_{k,j},\delta_{k,j})$ are $\mathbf{u}_{r,1}(\hat{\phi}_{k,j}) = [\cos\hat{\phi}_{k,j}, \sin\hat{\phi}_{k,j}]^{\mathrm{T}}$ and $\mathbf{u}_{r,2}(\hat{\phi}_{k,j}) = [-\sin\hat{\phi}_{k,j}, \cos\hat{\phi}_{k,j}]^{\mathrm{T}}$, with eigenvalues $\gamma_{k,j}^{(+)} = 1 - \sin\delta_{k,j} \ge 0$, and $\gamma_{k,j}^{(-)} = -\sin\delta_{k,j} \le 0$. However,

Algorithm 1 Robust Power Allocation

1: Set $m = 1$.
2: Determine an initial guess of $\{\mathbf{p}_j^{(m-1)}\}$ using the nominal values $\{\hat{\phi}_{k,j}, \hat{\mathbf{h}}_{k,j}\}$ (i.e., the non-robust power allocation).
3: Determine the worst-case channel deviation $\Delta\mathbf{h}_{k,j}^{\mathrm{ws}}$ for the current guess of $\{\mathbf{p}_j^{(m-1)}\}$.
4: Determine a pessimistic power allocation $\{\mathbf{p}_{\mathrm{pess},j}\}$, ignoring $\gamma_{k,j}^{(-)}$. Set $\{\mathbf{p}_j^{(m)} = \mathbf{p}_{\mathrm{pess},j}\}$.
5: Determine $\mathbf{X}_k(\{\mathbf{p}_j\})$ and $\Delta\mathbf{h}_{k,j}^{\mathrm{ws}}$ for the current guess of $\{\mathbf{p}_j^{(m)}\}$.
6: Determine a corrected power allocation $\{\mathbf{p}_j^{(m+1)} = \mathbf{p}_{\mathrm{corr},j}\}$, accounting for $\gamma_{k,j}^{(-)}$.
7: Set $m = m+1$ and go back to step 5 until $|\Delta P_{T,\mathrm{multi}}^{(m)}| \le \xi_{\mathrm{th}}$.

the worst-case channel depends on the power-allocation, and hence we have to resort to an iterative approach, outlined below.

In Algorithm 1, the worst-case channel deviation $\Delta\mathbf{h}_{k,j}^{\mathrm{ws}}$ is determined using a previously determined power allocation, and this power allocation is progressively refined. In what follows, we solve the robust power allocation for two sets of uncertainties on the channel coefficients, $\mathcal{H}_{k,j}^{(1)}$ and $\mathcal{H}_{k,j}^{(2)}$ from Section II-B, according to the above procedure.

B. Robust Power Allocation for $\Delta\mathbf{h}_{k,j} \in \mathcal{H}_{k,j}^{(1)}$

In this section, first we obtain the worst-case channel deviation $\Delta\mathbf{h}_{k,j}^{\mathrm{ws}}$ (step 3 in Algorithm 1) using an initial guess of $\{\mathbf{p}_j\}$ (step 2 in Algorithm 1). Second, a pessimistic power allocation is obtained based on the worst-case channel deviation (step 4 in Algorithm 1). Third, a corrected power allocation is designed by the inclusion of a PSD matrix in the SDP optimization based on the solution of the pessimistic power allocation and accounting for $\gamma_{k,j}^{(-)}$ (step 6 in Algorithm 1). The algorithm stops when the change in the used power is smaller than a predefined threshold ξ_{th} (step 7 in Algorithm 1).

1) Worst-Case Channel: The values of the channel coefficients that maximize the SPEB can be obtained by solving the following optimization problem.

$$\underset{\Delta\mathbf{h}_{k,j}\in\mathcal{H}_{k,j}^{(1)}}{\text{minimize}} \quad \lambda_{k,j}. \tag{28}$$

To solve (28), we propose the following proposition, requiring introduction of $\boldsymbol{\Omega}_j(\mathbf{p}_j) \triangleq \mathbf{M}_j^{(1)}(\mathbf{p}_j) - \mathbf{M}_j^{(2)}(\mathbf{p}_j)$.

Proposition 1: Solving (28) leads to

$$\Delta\mathbf{h}_{k,j}^{\mathrm{ws}}(\mathbf{p}_j) = -(\boldsymbol{\Omega}_j(\mathbf{p}_j) + \varrho_{k,j}\mathbf{I}_L)^{-1}\boldsymbol{\Omega}_j(\mathbf{p}_j)\hat{\mathbf{h}}_{k,j}, \tag{29}$$

in which $\varrho_{k,j}$ denotes the Lagrange multiplier associated with the constraint $\Delta\mathbf{h}_{k,j} \in \mathcal{H}_{k,j}^{(1)}$.

Proof: See Appendix B. ■

The value of $\varrho_{k,j}$ can be found numerically relying on the Karush-Kuhn-Tucker (KKT) conditions, as detailed in Appendix C. Substituting (29) into the definition of $\lambda_{k,j}$ (9) leads to the worst-case RII

$$\lambda_{k,j}^{\min} = \hat{\mathbf{h}}_{k,j}^{\mathrm{H}}\widetilde{\Lambda}_{k,j}^{\mathrm{H}}(\mathbf{p}_j)\boldsymbol{\Omega}_j(\mathbf{p}_j)\widetilde{\Lambda}_{k,j}(\mathbf{p}_j)\hat{\mathbf{h}}_{k,j}, \tag{30}$$

in which

$$\widetilde{\Lambda}_{k,j}(\mathbf{p}_j) = -\mathbf{U}_j(\mathbf{p}_j)(\Lambda_j(\mathbf{p}_j) + \varrho_{k,j}\mathbf{I}_L)^{-1}\Lambda_j(\mathbf{p}_j)\mathbf{U}_j^{\mathrm{H}}(\mathbf{p}_j) + \mathbf{I}_L,$$

with $\mathbf{U}_j(\mathbf{p}_j)$ and $\Lambda_j(\mathbf{p}_j)$ obtained by eigen-decomposition $\boldsymbol{\Omega}_j(\mathbf{p}_j) = \mathbf{U}_j(\mathbf{p}_j)\Lambda_j(\mathbf{p}_j)\mathbf{U}_j^{\mathrm{H}}(\mathbf{p}_j)$. It is clear that $\lambda_{k,j}^{\min}$ depends on $\mathbf{p}_j$ in such a way that $\bar{\mathbf{J}}_{e,k}(\{\mathbf{p}_j\}) \triangleq \sum_{j\in\mathcal{N}_b}\lambda_{k,j}^{\min}\mathbf{Q}_r(\hat{\phi}_{k,j},\delta_{k,j})$ can no longer be written as a linear function of the power (in contrast to the non-robust and designs with expectation constraints). This is the reason why we have to resort to the procedure in Algorithm 1.

2) Pessimistic Power Allocation: Given a guess of the power allocation and a corresponding guess of $\Delta\mathbf{h}_{k,j}^{\mathrm{ws}}$, we can express the current guess of the worst-case EFIM as $\bar{\mathbf{J}}_{e,k}(\{\mathbf{p}_j\}) = \hat{\mathbf{J}}_{e,k}(\{\mathbf{p}_j\}) + \mathbf{X}_k(\{\mathbf{p}_j\})$ in which $\hat{\mathbf{J}}_{e,k}(\{\mathbf{p}_j\})$ includes the $\mathbf{M}_j^{(1)}(\mathbf{p}_j)$-related part of the EFIM and the $\mathbf{M}_j^{(2)}(\mathbf{p}_j)$-related part of the EFIM corresponding to the positive eigenvalues $\gamma_{k,j}^{(+)}$, and the PSD matrix $\mathbf{X}_k(\{\mathbf{p}_j\})$ is the $\mathbf{M}_j^{(2)}(\mathbf{p}_j)$-related part of the EFIM corresponding to the negative eigenvalues $\gamma_{k,j}^{(-)}$, that is

$$\begin{aligned}\mathbf{X}_k(\{\mathbf{p}_j\}) = \zeta \sum_{j\in\mathcal{N}_b} |\gamma_{k,j}^{(-)}|\mathbf{u}_{r,2}(\hat{\phi}_{k,j})(\hat{\mathbf{h}}_{k,j} + \Delta\mathbf{h}_{k,j}^{\mathrm{ws}})^{\mathrm{H}} \\ \times\mathbf{M}_j^{(2)}(\mathbf{p}_j)(\hat{\mathbf{h}}_{k,j} + \Delta\mathbf{h}_{k,j}^{\mathrm{ws}})\mathbf{u}_{r,2}^{\mathrm{T}}(\hat{\phi}_{k,j}).\end{aligned} \tag{31}$$

Consequently, $\hat{\mathbf{J}}_{e,k}(\{\mathbf{p}_j\})$ can be decomposed as

$$\begin{aligned}\hat{\mathbf{J}}_{e,k}(\{\mathbf{p}_j\}) = \sum_{j\in\mathcal{N}_b}\widetilde{\nu}_{k,j}(\mathbf{p}_j)\mathbf{Q}_r(\hat{\phi}_{k,j},\delta_{k,j}) \\ - \widetilde{\Psi}_{k,j}^{\mathrm{H}}(\mathbf{p}_j)\Sigma^{-1}(\mathbf{p}_j)\widetilde{\Psi}_{k,j}(\mathbf{p}_j),\end{aligned} \tag{32}$$

with

$$\widetilde{\nu}_{k,j}(\mathbf{p}_j) = \zeta(\hat{\mathbf{h}}_{k,j} + \Delta\mathbf{h}_{k,j}^{\mathrm{ws}})^{\mathrm{H}}\mathbf{M}_j^{(1)}(\mathbf{p}_j)(\hat{\mathbf{h}}_{k,j} + \Delta\mathbf{h}_{k,j}^{\mathrm{ws}}), \tag{33}$$

$$\widetilde{\Psi}_{k,j}^{\mathrm{H}}(\mathbf{p}_j) = \sqrt{\zeta\gamma_{k,j}^{(+)}}\mathbf{u}_{r,1}(\hat{\phi}_{k,j})(\hat{\mathbf{h}}_{k,j} + \Delta\mathbf{h}_{k,j}^{\mathrm{ws}})^{\mathrm{H}}\,\Xi^{\mathrm{H}}(\mathbf{p}_j). \tag{34}$$

It is now clear that since $\bar{\mathbf{J}}_{e,k}(\{\mathbf{p}_j\}) \succeq \hat{\mathbf{J}}_{e,k}(\{\mathbf{p}_j\})$, a power allocation based on $\hat{\mathbf{J}}_{e,k}(\{\mathbf{p}_j\})$ will lead to an overly robust design (i.e., a pessimistic design). The constraint $\mathrm{tr}\{\hat{\mathbf{J}}_{e,k}^{-1}(\{\mathbf{p}_j\})\} \le \beta$ can be formulated as an SDP. This SDP (for a given value of $\Delta\mathbf{h}_{k,j}^{\mathrm{ws}}$) is of exactly the same form as the non-robust SDP (14a)–(18), but in $\widetilde{\Pi}_k(\{\mathbf{p}_j\},\widetilde{\mathbf{G}}_k)$ from (18), $\nu_{k,j}(\mathbf{p}_j)$ is replaced by $\widetilde{\nu}_{k,j}(\mathbf{p}_j)$, $\Psi_k^{\mathrm{H}}(\{\mathbf{p}_j\})$ is replaced by $\widetilde{\Psi}_k^{\mathrm{H}}(\{\mathbf{p}_j\})$ and $\mathbf{J}_r(\hat{\phi}_{k,j})$ is replaced by $\mathbf{Q}_r(\hat{\phi}_{k,j},\delta_{k,j})$. We denote the solution as $\{\mathbf{p}_{\mathrm{pess},j}\}$.

3) Corrected Power Allocation: For the same guess of $\Delta\mathbf{h}_{k,j}^{\mathrm{ws}}$, we now account for $\mathbf{X}_k(\{\mathbf{p}_{\mathrm{pess},j}\})$ to obtain a less conservative power allocation. This is achieved through the following optimization:

$$\mathcal{A}_{\mathrm{R}}^{\mathrm{SDP}}: \quad \underset{\{\mathbf{p}_j\},\{\widetilde{\mathbf{G}}_k\}}{\text{minimize}} \quad \sum_{j\in\mathcal{N}_b}\mathbf{1}^{\mathrm{T}}\mathbf{p}_j \tag{35a}$$

$$\text{subject to } \widetilde{\Theta}(\widetilde{\mathbf{G}}_k;\beta) \succeq \mathbf{0}, \quad \forall k\in\mathcal{N}_a \tag{35b}$$

$$\widetilde{\Pi}_k(\{\mathbf{p}_j\},\widetilde{\mathbf{G}}_k;\mathbf{X}_k(\{\mathbf{p}_{\mathrm{pess},j}\})) \succeq \mathbf{0}, \tag{35c}$$

$$\mathbf{p}_j \succeq \mathbf{0}, \quad \forall j\in\mathcal{N}_b \tag{35d}$$

TABLE I

APPROXIMATE COMPLEXITY COMPARISON OF THE NON-ROBUST, POWER ALLOCATIONS WITH EXPECTATION AND ROBUSTNESS CONSTRAINTS, FOR N SUBCARRIERS, L-PATH CHANNELS, N_a AGENTS, N_b ANCHORS, M_q SAMPLES, AND $M^{\max}$ ITERATIONS IN ALGORITHM 1

	number of Newton steps	Newton step complexity
non-robust	$\sqrt{(N_aL+N)N_b}$	$N_aN_b^2L^2(N_bL+N)+N^3N_b$
expectation	$\sqrt{M_qN_bN_aL+NN_b}$	$M_qN_aN_b^2L^2(N_bL+N)+M_q^3N_a+N^3N_b$
robust	$M^{\max}\sqrt{(N_aL+N)N_b}$	$N_aN_b^2L^2(N_bL+N)+N^3N_b$

in which $\widetilde{\mathbf{G}}_k$ is an auxiliary matrix, $\widetilde{\Theta}(\widetilde{\mathbf{G}}_k;\beta)$ was defined in (17), and

$$\widetilde{\Pi}_k(\{\mathbf{p}_j\},\widetilde{\mathbf{G}}_k;\mathbf{X}_k(\{\mathbf{p}_{\text{pess},j}\})) = \begin{bmatrix} \mathbf{S}(\{\mathbf{p}_j\};\{\mathbf{p}_{\text{pess},j}\})-\widetilde{\mathbf{G}}_k & \widetilde{\Psi}_k^{\mathrm{H}}(\{\mathbf{p}_j\}) \\ \widetilde{\Psi}_k(\{\mathbf{p}_j\}) & \Sigma(\{\mathbf{p}_j\}) \end{bmatrix}, \quad (36)$$

where $\mathbf{S}(\{\mathbf{p}_j\};\{\mathbf{p}_{\text{pess},j}\}) = \sum_{j\in\mathcal{N}_b}\widetilde{\nu}_{k,j}(\mathbf{p}_j)\mathbf{Q}_r(\hat{\phi}_{k,j},\delta_{k,j}) + \mathbf{X}_k(\{\mathbf{p}_{\text{pess},j}\})$. The solution to $\mathcal{A}_{\mathrm{R}}^{\mathrm{SDP}}$ will be denoted by $\{\mathbf{p}_{\text{corr},j}\}$. Note that the inclusion of the PSD matrix $\mathbf{X}_k(\{\mathbf{p}_{\text{pess},j}\})$ in (35c) will lead to a reduction in the allocated power, i.e., $\sum_{j\in\mathcal{N}_b}\mathbf{1}^{\mathrm{T}}\mathbf{p}_{\text{corr},j} \leq \sum_{j\in\mathcal{N}_b}\mathbf{1}^{\mathrm{T}}\mathbf{p}_{\text{pess},j}$.

4) Complete Iterative Procedure: The complete procedure proceeds as outlined in Algorithm 1. Starting from an initial guess of the power allocation, the $\Delta\mathbf{h}_{k,j}^{\text{ws}}$ is determined (see Section V-B.1). Then a conservative power allocation is determined (see Section V-B.2), followed by a correction (see Section V-B.3). Then the entire procedure (Section V-B.1 and Section V-B.3) is repeated until a measure of convergence is achieved. In our case, we consider the absolute value of the relative change of the total power

$$|\Delta P_{T,\text{multi}}^{(m)}| \triangleq \frac{|P_{T,\text{multi}}^{(m+1)}-P_{T,\text{multi}}^{(m)}|}{P_{T,\text{multi}}^{(m)}},$$

with $P_{\text{T,multi}}^{(m)} = \sum_{j\in\mathcal{N}_b}\mathbf{1}^{\mathrm{T}}\mathbf{p}_j^{(m)}$ to be smaller than a given threshold ξ_{th}, i.e., $|\Delta P_{T,\text{multi}}^{(m)}| \leq \xi_{\text{th}}$.

C. Robust Power Allocation for $\Delta\mathbf{h}_{k,j}\in\mathcal{H}_{k,j}^{(2)}$

1) Worst-Case Channel: The worst-case channel for $\Delta\mathbf{h}_{k,j}\in\mathcal{H}_{k,j}^{(2)}$ is found by solving

$$\underset{\Delta\mathbf{h}_{k,j}\in\mathcal{H}_{k,j}^{(2)}}{\text{minimize}} \quad \lambda_{k,j}. \quad (37)$$

The optimization problem (37) is formed by a quadratic cost function with linear constraints. This type of problems have no closed-form solution, but it is well-known that it can be solved with the simplex method, interior-point methods (IPMs), or it can be transformed to SDP and solved as an SDP [16].

2) Pessimistic and Corrected Power Allocations: Similar to Section V-B.2 and Section V-B.3, we can follow the same iterative procedure from Algorithm 1.

Remark: Computational Complexity

The complexity of each of the methods can be determined through an analysis based on the extension of the barrier methods with the general inequality constraints [16]. The result, expressed in terms of the number of Newton steps and the complexity per Newton step, is detailed in Table I. We note that with respect to the non-robust allocation, the allocation with expectation constraints has a complexity that is around $M_q^{1.5}$ times higher, while the robust allocation has a complexity around $M^{\max}$ times higher. Finally, the complexity of the robust allocation with the CSM grows linearly with the number of samples $M^{\max}$ in the channel uncertainty set in each iteration compared to the proposed algorithm, i.e., $M^{\max}$ multiplied by the Newton step complexity of the proposed robust solution.

VI. SIMULATION RESULTS

In this section, we compare the performance of the non-robust designs and proposed designs with expectation and robustness constraints in terms of the total allocated power, as well as the distribution of the power across subcarriers, and the SPEB performance.

A. Simulation Setup

We consider a network with $N_b = 4$ anchors and $N_a = 4$ agents. Each agent has a nominal position and nominal channel to each of the anchors. Due to, for instance, movement, the agents' positions and the channels become uncertain. The possible positions after movement are within an uncertainty disk with radius $\Delta r = 40$ m around the nominal positions $\mathbf{q}_k$ [m] $\in \{[\pm166.7 \ \pm 166.7]^{\mathrm{T}}\}$ for $k\in\{1,2,3,4\}$, as shown in Fig. 2. This position uncertainty then translates to angle uncertainty with $\Delta\phi_{k,j}\in[-\delta_{k,j},+\delta_{k,j}]$, which is obtained using simple trigonometric calculations. For the signals, we set[2] $N/T = 10$ MHz, and $N = 32$ subcarriers. All channels have $L = 5$ taps. Examples of the magnitude of channel frequency response associated with the nominal channels $\hat{\mathbf{h}}_{k,j}$ generated randomly as $\mathcal{CN}(0,5\mathbf{I}_L)$ from anchor 7 to all four agents are presented in Fig. 3 (top). Channel uncertainties are generated from the uncertainty region based on H1 with $\epsilon = 0.6$ visualized in the frequency domain in Fig. 3 (bottom). To evaluate the different power allocations, we consider $N_q = 150$ possible channel and position realizations. Finally, we set the SPEB threshold $\sqrt{\beta} = \sqrt{0.5} = 0.7071$ m and define the maximum constraint violation

$$\mathcal{V}^{\max}(\{\mathbf{p}_j\}) \triangleq \sqrt{\mathcal{P}^{\max}(\{\mathbf{p}_j\})}-\sqrt{\beta},$$

where

$$\mathcal{P}^{\max}(\{\mathbf{p}_j\}) \triangleq \max_{k=1,\ldots,N_a}\mathcal{P}_k^{\max}(\{\mathbf{p}_j\}).$$

[2]The most usual working modes of long term evolution (LTE) are based on the 5 MHz and 10 MHz operating bandwidth [17], [18]. Thus, we have chosen 10 MHz operating bandwidths in order to represent usual LTE positioning conditions.

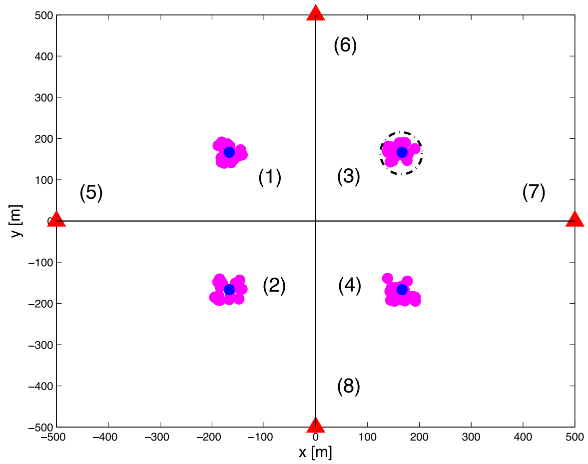

Fig. 2. Network topology with four anchors (red triangles) and four agents (blue dots) over the 1000 m × 1000 m map. The pink dots represent possible positions due to uncertainty, and the dash-dot circle denotes the uncertainty disk.

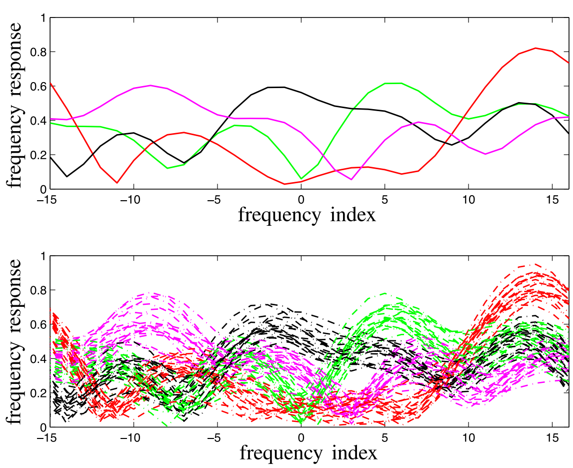

Fig. 3. Magnitude of the frequency response for channels between anchor $k = 7$ and the agents: nominal response $|\mathbf{F}_L \hat{\mathbf{h}}_{k,j}|$ (top), response with channel uncertainty $|\mathbf{F}_L(\hat{\mathbf{h}}_{k,j}+\Delta\mathbf{h}_{k,j})|$ (bottom).

We have considered five power allocation approaches:

- *Benchmark:* Power allocation is based on the true positions and channel coefficients after the movement. This is (14a)–(14c) using the actual value of the channel and agents' positions. Note that this strategy is not causal, as it relies on the positions after movement.
- *Non-robust:* Power allocation is based on the SDP form of problem $\mathcal{A}_{\mathrm{NR}}$ in (14a)-(14c), using the nominal positions and nominal channels. Note that the resulting allocation may violate the SPEB constraint when evaluated in the true positions with the true channels.
- *Expectation:* Power allocation is based on $\mathcal{A}_{\mathrm{E}}$ in (19a)–(19c) with the SDP reformulation of (23a)–(23d) for M_q realizations of channel coefficients and positions after movement. We have found that $M_q = 25$ is sufficient (i.e., power allocations do not change significantly for $M_q > 25$) and we use this value for the remainder of the paper.

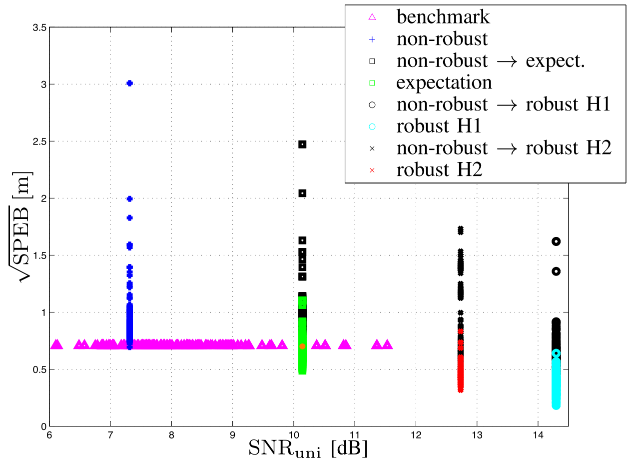

Fig. 4. Unicast: SPEB after movement vs SNR for 150 channel and position values due to uncertainty after movement. The benchmark exhibits fixed SPEB but a different power per realization. The proposed methods are designed taking into account the uncertainty in the channels and agents' positions, and thus exhibit a fixed SNR, but varying SPEB. The arrows $A \rightarrow B$ indicate that the allocation A was used, but the power of all the subcarriers is multiplied by a constant so as to obtain the same total power as with allocation B.

- *Robust H1:* Power allocation is based on the solution of the problem $\mathcal{A}_{\mathrm{R}}$ in (26a)–(26c) with channel uncertainties modeled to belong to $\mathcal{H}^{(1)}_{k,j}$.
- *Robust H2:* Power allocation is based on the solution of the problem $\mathcal{A}_{\mathrm{R}}$ in (26a)–(26c) with channel uncertainties modeled to belong to $\mathcal{H}^{(2)}_{k,j}$. The upper bound on the per-channel tap uncertainty is set to $\epsilon_l = \epsilon/\sqrt{L}$, so that $\mathcal{H}^{(1)}_{k,j} \supset \mathcal{H}^{(2)}_{k,j}$.

For each of these power allocations, we determine the total power as well as the actual SPEB for $N_q = 150$ realizations of the channels and agents' positions after movement. In addition, we also evaluate the SPEB of the non-robust approach when the power is increased to the same level as the approaches with expectation and robustness constraints. The SDPs and convex programs are solved using CVX [19].

B. Results and Discussion

Total Allocated Power: Fig. 4–5 show the result for unicast and multicast transmissions, respectively. In these plots, we show the SPEB vs $\mathrm{SNR_{uni}} = P_{\mathrm{T,uni}}/\sigma_w^2$ and $\mathrm{SNR_{multi}} = P_{\mathrm{T,multi}}/\sigma_w^2$ in which $P_{\mathrm{T,uni}} = \sum_{k\in\mathcal{N}_a}\sum_{j\in\mathcal{N}_b} \mathbf{1}^{\mathrm{T}}\mathbf{p}_{k,j}$ and $P_{\mathrm{T,multi}} = \sum_{j\in\mathcal{N}_b} \mathbf{1}^{\mathrm{T}}\mathbf{p}_j$. The performance of each method for different channels and positions after the agents' movement within the uncertainty regions is investigated. The goal is to show the importance of considering the channel and position uncertainty for the power allocation in terms of increasing the total power and the SPEB for unicast and multicast transmissions.

For the unicast scenario (Fig. 4), the non-causal benchmark method leads to an $\sqrt{\mathrm{SPEB}}$ of exactly 0.7071 m, while the non-robust solution has a fixed power allocation, leading to widely varying SPEB, depending on the positions and channels after movement. We note that for all the 150 channels and positions under evaluation, the SPEB constraint is violated by the

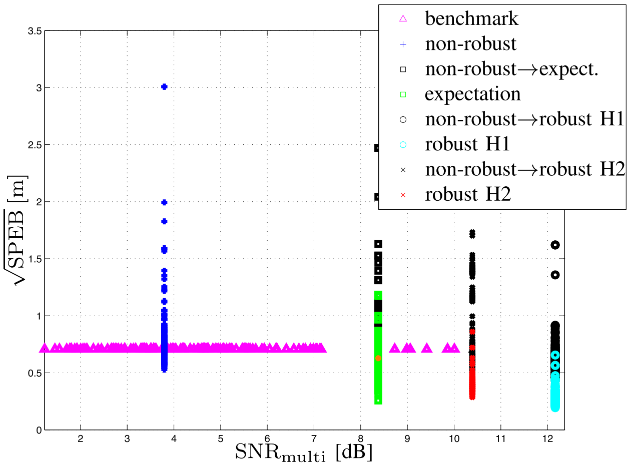

Fig. 5. Multicast: SPEB after movement vs SNR for 150 channel and position values after movement. The benchmark exhibits fixed SPEB but a different power per realization. The proposed methods are designed taking into account the uncertainty in the channels and agents' positions, and thus exhibit a fixed SNR, but varying SPEB. The arrows $A \rightarrow B$ indicate that the allocation A was used, but the power of all the subcarriers is multiplied by a constant so as to obtain the same total power as with allocation B.

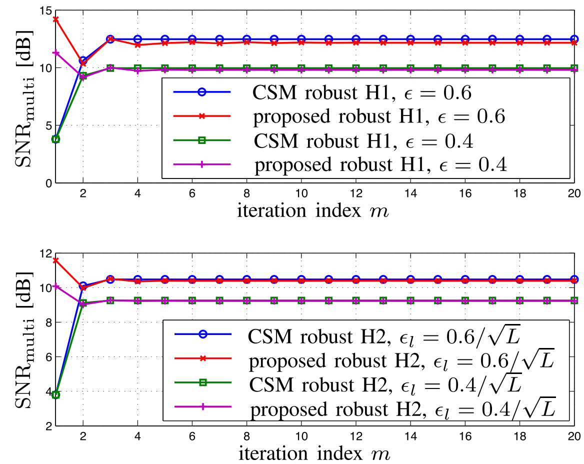

Fig. 6. Evolution of $\text{SNR}_{\text{multi}}$ for (top) robust H1 and (bottom) robust H2 based on the proposed algorithm and on the CSM with $\epsilon = \{0.6, 0.4\}$ and $\epsilon_l = \epsilon/\sqrt{L}$.

non-robust power allocation. The allocation with expectation constraints requires slightly more power than the non-robust design, but leads to a lower SPEB, with an average around the target value of $\sqrt{\beta} = 0.7071$ m. Scaling up the power in the non-robust design to a total level equal to the design with expectation constraints leads to a slight improvement in the SPEB (represented with the black markers in Fig. 4), but is still much worse than the design with expectation constraints in terms of the average SPEB. To show the performance of the design with expectation constraints using the sampling average in (20), the mean value of the SPEB using the design with the sampling average is shown by the orange '*' on top of the green squares. It can be observed that using the design with the sampling average in (20), the resulting allocation very likely fulfills (19b) with the desired localization accuracy of $\sqrt{\beta} = 0.7071$ m. The approximate performance of the mean value of the sample average close to the desired accuracy of $\sqrt{\beta} = 0.7071$ m can be justified using the sample average approximation for stochastic programming problems [20]. The two robust designs require even more power, but are able to meet the SPEB requirement for each realization of the channels and positions after movement based on H1 channel uncertainty. We note that the robust H1 approach requires more power than the robust H2 approach, what is logical given that for the selected ϵ and ϵ_l the H1 uncertainty region is larger than H2. This leads to the fact that the robust H2 for some values after the agent movement slightly violates the benchmark $\sqrt{\beta} = 0.7071$ m due to the fact that the upper bound on the per-channel tap uncertainty is set to $\epsilon_l = \epsilon/\sqrt{L}$, so that $\mathcal{H}_{k,j}^{(1)} \supset \mathcal{H}_{k,j}^{(2)}$. As with the approach with expectation constraints, scaling up the power of the non-robust approach to the level of the robust approaches still violates the SPEB constraint. This means that simply increasing the power is not an efficient way to fulfill the SPEB bound in the presence of channel and position uncertainty, and that the inclusion of the uncertainty in the design itself is fundamental to achieve a given performance without paying an excessive penalty in power. For the multicast scenario (Fig. 5), we observe similar trends. Interestingly, for all allocations, the total required power for different power allocation methods in unicast transmission is less than $N_a = 4$ times the total power in multicast transmission. This is due to the fact that while unicast requires more transmissions, each transmission can be optimized (in terms of total power and per-subcarrier allocation) for each individual agent. Fig. 6–7 show the convergence of the optimization solution and the maximum constraint violation $\mathcal{V}^{\max}(\{\mathbf{p}_j\})$ with our algorithm and the CSM for the uncertainty sets $\mathcal{H}_{k,j}^{(1)}$ and $\mathcal{H}_{k,j}^{(2)}$ with the upper bounds $\epsilon = \{0.6, 0.4\}$ and $\epsilon_l = \epsilon/\sqrt{L}$ and multicast transmission. It turns out that after a few iterations, the proposed algorithm exhibits similar performance to the solution obtained by the CSM. Starting from the nominal values of the channel coefficients and the agents' positions both algorithms converge to very similar solutions. Specifically, for the uncertainty sets $\mathcal{H}_{k,j}^{(1)}$ and $\mathcal{H}_{k,j}^{(2)}$ with the upper bounds $\epsilon = \{0.6, 0.4\}$ and $\epsilon_l = \epsilon/\sqrt{L}$, there is a small gap $\Delta P_{\text{T,multi}}$ [dB] $= \{0.3, 0.15\}$ (for robust H1) and $\Delta P_{\text{T,multi}}$ [dB] $= \{0.1, 0.025\}$ (for robust H2). This leads to a small deviation from $\sqrt{\beta} = \sqrt{0.5} = 0.7071$ m of the order of $\mathcal{V}^{\max}(\{\mathbf{p}_j\})$ [cm] $= \{1.45, 0.161\}$ (robust H1) and $\mathcal{V}^{\max}(\{\mathbf{p}_j\})$ [cm] $= \{0.064, 0.013\}$ (robust H2). Consequently, the maximum constraint violation $\mathcal{V}^{\max}(\{\mathbf{p}_j\})$ is very small compared to the target accuracy $\sqrt{\beta}$.

Power Across Subcarriers: We analyze the per-carrier allocation for robust H1 case since the same argument can be made for the other allocations. Fig. 8 shows the normalized per-carrier allocations for multicast and unicast transmissions together with non-robust allocations. We observe that subcarriers at the edges are used in all (i.e., robust and non-robust) allocations (as also observed in [12]), while for other subcarriers, robust and non-robust designs allocate power to different subcarriers. This justifies the fact that a scaling of the total power for the non-robust design cannot achieve the

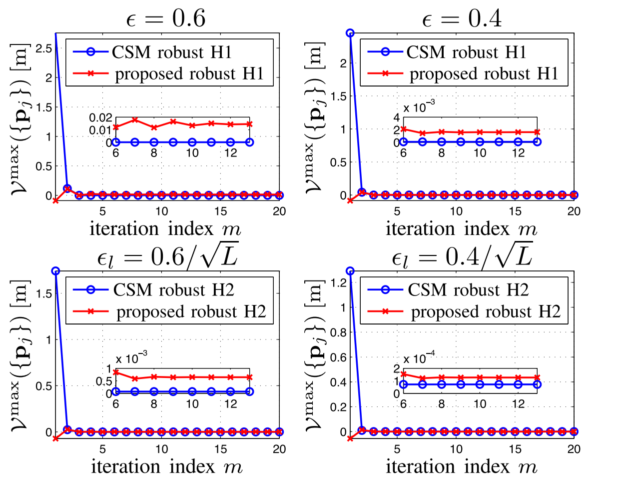

Fig. 7. Evolution of $\mathcal{V}^{\max}(\{\mathbf{p}_j\})$ for (top) robust H1 and (bottom) robust H2 based on the proposed algorithm and on the CSM with $\epsilon = \{0.6, 0.4\}$ and $\epsilon_l = \epsilon/\sqrt{L}$.

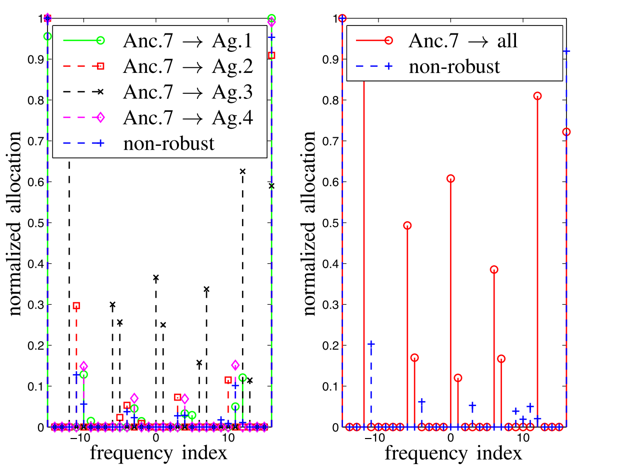

Fig. 8. Robust H1 power allocation based on (left) unicast transmission and (right) multicast transmission for anchor 7.

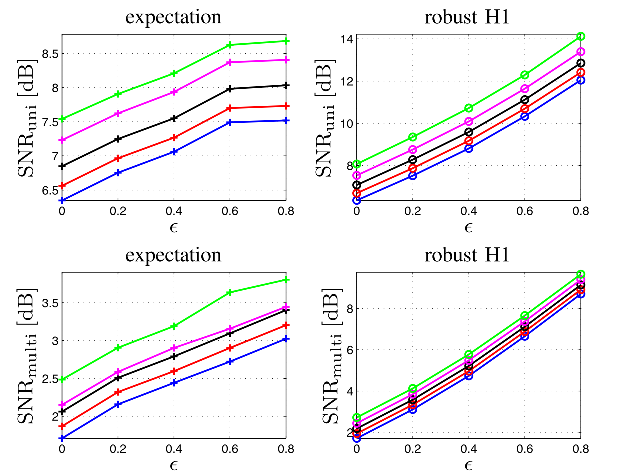

Fig. 9. Required SNR with respect to channel uncertainty H1 and location uncertainty with Δr [m] $\in$ {0(blue), 10(red), 20(black), 30(pink), 40(green)} for (top) unicast and (bottom) multicast transmissions and $\sqrt{\beta} = 0.7071$ m.

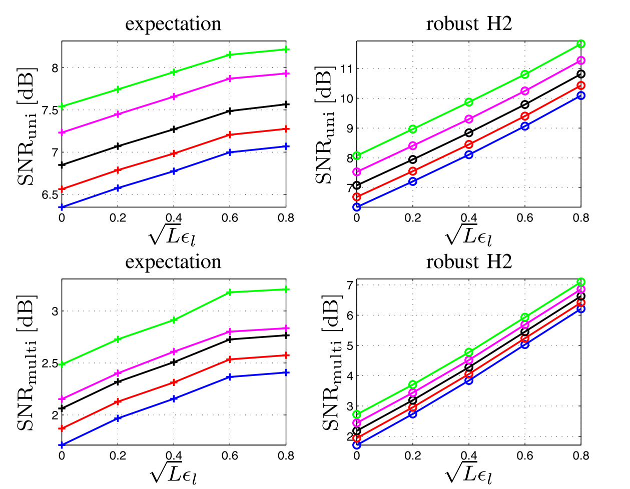

Fig. 10. Required SNR with respect to channel uncertainty H2 and location uncertainty with Δr [m] $\in$ {0(blue), 10(red), 20(black), 30(pink), 40(green)} for (top) unicast and (bottom) multicast transmissions and $\sqrt{\beta} = 0.7071$ m.

same performance as the proposed designs. Moreover, the unicast transmission allows different power across subcarriers to achieve the desired value of SPEB for each agent. This is the main reason why the total power increase for unicast transmission is less than $N_a = 4$ times the total power for their multicast counterparts. Finally, it is worth mentioning that the similarity between robust designs increases by reducing the number of channel taps L. Particularly, using $L = 1$ the performance of the robust designs with the assumptions H1 and H2 would be the same, since the channel vector reduces to a scalar.

Performance of the Allocations for Different Uncertainties: In Fig. 9–11, we investigate the performance of proposed allocations for $\sqrt{\beta} = 0.7071$ m with different uncertainties on the channel coefficients ϵ, $\epsilon_l = \epsilon/\sqrt{L}$, and Δr [m] $\in$ $\{0, 10, 20, 30, 40\}$ for multicast and unicast transmissions. In general, the required SNR for proposed designs increases by increasing the channel and/or location uncertainties. From Fig. 9–10, we observe that by going from $\Delta r = 0$ m to $\Delta r = 40$ m for $\epsilon = \sqrt{L}\epsilon_l = 0.6$, the required increase of the SNR is approximately 2 dB for unicast and 1 dB for multicast with robust H1 and robust H2 allocations. For the design with expectation constraints, by going from $\Delta r = 0$ m to $\Delta r = 40$ m for $\epsilon = \sqrt{L}\epsilon_l = 0.6$, the required increase of the SNR is approximately 1.1 dB for unicast and 0.9 dB for multicast under H1 uncertainty, and 1.15 dB for unicast and 0.8 dB for multicast under H2 uncertainty. Moreover, the required increase of the SNR for the robust designs based on channel uncertainties for a given location uncertainty is around 6 dB for robust H1, 4 dB for robust H2, and 1dB for H1 and H2 with expectation constraints, with multicast and unicast transmissions. From Fig. 11, it is observed that the maximum increase of the required SNR by only considering the effect of location uncertainty (i.e., $\epsilon = \sqrt{L}\epsilon = 0$) is around 2.3 dB for robust design and 1.2 dB for design with expectation constraints, with unicast transmission, and around 1.4 dB and 0.8 dB with multicast transmission. From the above observations, we conclude that the increase of the required SNR based on the location uncertainty for a given

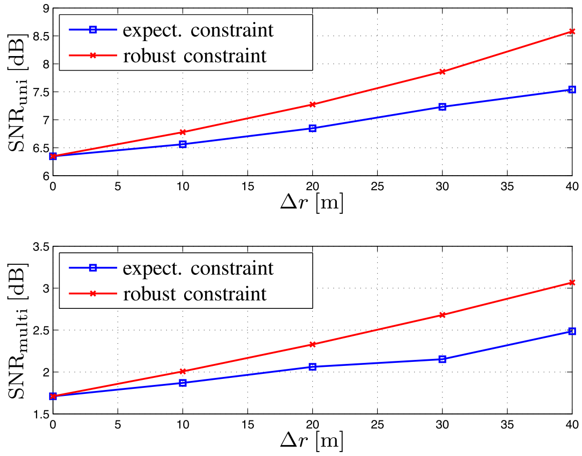

Fig. 11. Required SNR with respect to location uncertainty Δr[m] with $\epsilon = 0$ for (top) unicast and (bottom) multicast transmissions and $\sqrt{\beta} = 0.7071$ m.

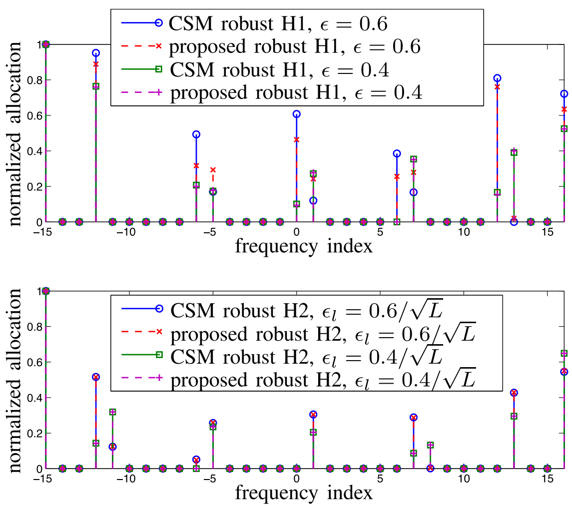

Fig. 12. Robust (top) H1 and (bottom) H2 power allocations based on the proposed algorithm and the CSM after convergence with $\epsilon = \{0.6, 0.4\}$ and $\epsilon_l = \epsilon/\sqrt{L}$.

channel uncertainty is much smaller than the increase of the required SNR based on channel uncertainty for a given location uncertainty especially for the robust designs.

Fig. 12 shows the power allocation after convergence for the proposed algorithm and the CSM, respectively, for the same conditions as in Fig. 6–7. We observe that both methods obtain a similar power allocation, especially for the robust H2 case and the robust H1 with $\epsilon = 0.4$.

Comparison With Single-Carrier Allocations: Finally, we compare the non-robust and proposed designs in single-carrier transmissions with their multi-carrier counterparts. The EFIM for the position of kth agent with single-carrier allocation is given by [9]

$$\mathbf{J}_e(\mathbf{q}_k) = \sum_{j \in \mathcal{N}_b} \xi_{k,j}\, p_{k,j}\, \mathbf{J}_r(\phi_{k,j}),$$

where $p_{k,j}$ denotes the transmitted power from anchor j to agent k,

$$\xi_{k,j} = \frac{8\pi^2 W^2}{c^2}(1 - \chi_{k,j})\frac{|\alpha_{k,j,1}|^2}{\sigma_w^2},$$

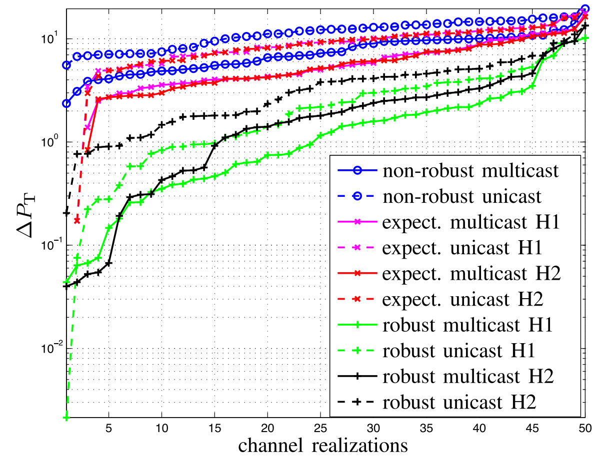

Fig. 13. Relative change of total power in single-carrier vs multi-carrier designs for different allocations.

where $W = N/T$ is the effective bandwidth, $\chi_{k,j}$ denotes the path-overlap coefficient, and $\alpha_{k,j,1}$ is the complex channel gain of the first path. To make the comparison with multi-carrier transmission possible, we set $|\alpha_{k,j,1}|^2 = \|\mathbf{h}_{k,j}\|^2$ and $\chi_{k,j} = 0$. Although this value of $\chi_{k,j}$ makes the comparison slightly optimistic for single-carrier transmission since the partial overlap of the L paths considered in the multi-carrier case could increase the value of $\chi_{k,j}$, this is considered acceptable given that the goal is to show the advantage of multi-carrier power allocation for localization. Fig. 13 shows the relative total power increase $\Delta P_{\mathrm{T}} = (P_{\mathrm{T,sc}} - P_{\mathrm{T,mc}})/P_{\mathrm{T,mc}}$ in single-carrier transmission (with power $P_{\mathrm{T,sc}}$) compared to multi-carrier designs (with power $P_{\mathrm{T,mc}}$) for the different allocations and 50 channel realizations. For visualization purposes, the powers have been sorted. The average relative power increases for multicast are 7.8 (non-robust), 6.1 and 5.9 (expect. H1 and expect. H2), and 1.9 and 2.5 (robust H1 and robust H2, respectively). For the unicast scenario, these gains increase with an additional 50% for each approach. In general we observe that multi-carrier transmission requires less power than single-carrier transmission to achieve a given localization accuracy, but this gain diminishes with increased robustness.

VII. Conclusion

We have addressed the problem of power allocation for network localization under uncertainty in both channel and user locations. We considered per-channel tap and norm-based uncertainty. We first proposed a non-robust design based on perfect network parameters for OFDM-based positioning via SDP programming. To consider channel and location uncertainties, power allocations with expectation and robustness constraints of the SPEB for OFDM-based positioning with multicast and unicast transmission have been developed. We have observed that proposed designs outperform the non-robust designs even by increasing the total power of the non-robust design uniformly to the level of the proposed allocations. Moreover, we showed that compared with location uncertainty, channel uncertainty considerably affects the required SNR especially for the robust design. Finally, we observed that the total required power for multi-carrier designs was less than their single-carrier counterparts.

Appendix A
Proof of $\Phi(\mathbf{x}_k, \mathbf{y}_m) = \mathbf{0}$ for $k \neq m$

The terms $\Phi(\boldsymbol{\theta}_k, \boldsymbol{\theta}_m)$, $\Phi(\mathbf{q}_k, \mathbf{q}_m)$, $\Phi(\boldsymbol{\theta}_m, \mathbf{q}_k)$, and $\Phi(\mathbf{q}_k, \boldsymbol{\theta}_m)$ are zero for $k \neq m$. We start with $\Phi(\boldsymbol{\theta}_k, \boldsymbol{\theta}_m)$, and continue with $\Phi(\mathbf{q}_k, \mathbf{q}_m)$ and $\Phi(\boldsymbol{\theta}_m, \mathbf{q}_k)$. By definition, we have

$$\Phi(\boldsymbol{\theta}_k, \boldsymbol{\theta}_m) = \frac{2}{\sigma_w^2} \Re \left\{ \frac{\partial \boldsymbol{\mu}^{\mathrm{H}}}{\partial \boldsymbol{\theta}_k} \frac{\partial \boldsymbol{\mu}}{\partial \boldsymbol{\theta}_m} \right\}, \tag{38}$$

where $\boldsymbol{\mu}$ is defined as

$$\boldsymbol{\mu} = \left[\boldsymbol{\mu}_1^{\mathrm{T}}, \ldots, \boldsymbol{\mu}_{N_a}^{\mathrm{T}}\right]^{\mathrm{T}}, \tag{39}$$

in which

$$\boldsymbol{\mu}_k = \left[\boldsymbol{\mu}_{k,N_a+1}^{\mathrm{T}}, \ldots, \boldsymbol{\mu}_{k,N_a+N_b}^{\mathrm{T}}\right]^{\mathrm{T}}, \tag{40}$$

and $\boldsymbol{\mu}_{k,j} = \Gamma(t_{k,j})\mathbf{B}_j \mathbf{F}_L \mathbf{h}_{k,j}$. Taking the derivative of $\boldsymbol{\mu}^{\mathrm{H}}$ with respect to $\boldsymbol{\theta}_k$ leads to

$$\frac{\partial \boldsymbol{\mu}^{\mathrm{H}}}{\partial \boldsymbol{\theta}_k} = \left[\tfrac{\partial \boldsymbol{\mu}_1^{\mathrm{H}}}{\partial \boldsymbol{\theta}_k}, \ldots, \tfrac{\partial \boldsymbol{\mu}_k^{\mathrm{H}}}{\partial \boldsymbol{\theta}_k}, \ldots, \tfrac{\partial \boldsymbol{\mu}_{N_a}^{\mathrm{H}}}{\partial \boldsymbol{\theta}_k}\right]. \tag{41}$$

The only non-zero element in (41) is the term $\partial \boldsymbol{\mu}_k^{\mathrm{H}} / \partial \boldsymbol{\theta}_k$, while the only non-zero element of $\partial \boldsymbol{\mu} / \partial \boldsymbol{\theta}_m$ is the term $\partial \boldsymbol{\mu}_m / \partial \boldsymbol{\theta}_m$. So, the multiplication of these terms is zero for $k \neq m$. A similar argument can be made for the terms $\Phi(\mathbf{q}_k, \mathbf{q}_m)$, $\Phi(\boldsymbol{\theta}_m, \mathbf{q}_k)$, and $\Phi(\mathbf{q}_k, \boldsymbol{\theta}_m)$.

Appendix B
Proof of Proposition 1

The Lagrangian associated with the optimization problem (28) can be expressed as

$$\begin{aligned}\mathcal{L}(\Delta\mathbf{h}_{k,j}; \varrho_{k,j}) = (\hat{\mathbf{h}}_{k,j} + \Delta\mathbf{h}_{k,j})^{\mathrm{H}} \boldsymbol{\Omega}_j(\mathbf{p}_j)(\hat{\mathbf{h}}_{k,j} + \Delta\mathbf{h}_{k,j}) \\ + \varrho_{k,j}(\|\Delta\mathbf{h}_{k,j}\|^2 - \epsilon^2),\end{aligned} \tag{42}$$

with the Lagrange multiplier $\varrho_{k,j} \geq 0$. The KKT conditions provide necessary and sufficient conditions for convex optimization problems. From the KKT conditions, the Lagrangian equation is

$$\boldsymbol{\nabla}_{\Delta\mathbf{h}_{k,j}} \mathcal{L}(\Delta\mathbf{h}_{k,j}; \varrho_{k,j}^{\mathrm{ws}}) \mid_{\Delta\mathbf{h}_{k,j}^{\mathrm{ws}}} = \mathbf{0}. \tag{43}$$

Using the Lagrangian equation (43), we obtain (29).

Appendix C
Numerical Solution for $\varrho_{k,j}$

To obtain the Lagrange multiplier $\varrho_{k,j}$ for a given value of $\mathbf{p}_j$, we use the Lagrangian equation

$$\frac{\partial}{\partial \varrho_{k,j}} \mathcal{L}(\Delta\mathbf{h}_{k,j}^{\mathrm{ws}}; \varrho_{k,j}) \mid_{\varrho_{k,j}^{\mathrm{ws}}} = 0. \tag{44}$$

This leads to

$$\|\Delta\mathbf{h}_{k,j}^{\mathrm{ws}}\|^2 = \epsilon^2. \tag{45}$$

Replacing (29) in (45) and the eigen-decomposition $\boldsymbol{\Omega}_j(\mathbf{p}_j) = \mathbf{U}_j(\mathbf{p}_j)\Lambda_j(\mathbf{p}_j)\mathbf{U}_j^{\mathrm{H}}(\mathbf{p}_j)$ with $\Delta\mathbf{g}_{k,j} = \mathbf{U}_j^{\mathrm{H}}(\mathbf{p}_j)\Delta\mathbf{h}_{k,j}$ and $\hat{\mathbf{g}}_{k,j} = \mathbf{U}_j^{\mathrm{H}}(\mathbf{p}_j)\hat{\mathbf{h}}_{k,j}$ results:

$$\sum_{l=1}^{L} \frac{\gamma_{j,l}^2}{(\gamma_{j,l} + \varrho_{k,j}^{\mathrm{ws}})^2} |\hat{g}_{k,j,l}|^2 = \epsilon^2, \tag{46}$$

in which $\gamma_{j,l}$ is the lth entry of the diagonal matrix of the eigenvalues $\Lambda_j(\mathbf{p}_j)$ and $\hat{g}_{k,j,l}$ denotes the lth element of $\hat{\mathbf{g}}_{k,j}$. In principle, (46) can be efficiently solved using Newton's method. Among the roots of (46), we choose the one that results the smallest value of the cost function $\lambda_{k,j}$. Note that $\varrho_{k,j}$ cannot be zero as it results $\lambda_{k,j}^{\min} = 0$. Moreover, since the Newton's method requires the initial value for the Lagrange multiplier $\varrho_{k,j}$, we present the following proposition that provides the necessary condition on the value of $\varrho_{k,j}$ to fulfill (46) and apply it as the initial value for the Newton's method.

Proposition 2: A necessary condition on $\varrho_{k,j}$ to fulfill (46) is $\varrho_{k,j} > \varrho_{k,j}^{\max}$ where

$$\varrho_{k,j}^{\max} = \max_{l} \left(\frac{\gamma_{j,l}|\hat{g}_{k,j,l}|}{\epsilon} - \gamma_{j,l} \right) . \forall l \in \{1, \ldots, L\} \tag{47}$$

Proof: For $\forall m$, (46) can be written as

$$\begin{aligned}\left(\gamma_{j,m}^2 |\hat{g}_{k,j,m}|^2 - \epsilon^2(\gamma_{j,m} + \varrho_{k,j})^2\right) \prod_{i \neq m} (\gamma_{j,i} + \varrho_{k,j})^2 \\ + \sum_{n \neq m} \gamma_{j,n}^2 |\hat{g}_{k,j,n}|^2 \prod_{i \neq n} (\gamma_{j,i} + \varrho_{k,j})^2 = 0.\end{aligned}$$

Using the fact that $\gamma_{j,l} \geq 0$ with at least two non-zero values since the minimum number of pilots to minimize $\lambda_{k,j}$ is $L+1$ and $\varrho_{k,j} > 0$, the necessary condition for the above equality to hold is to have negative term in parentheses for $m \in \{1, \ldots, L\}$. This requires $\varrho_{k,j}$ to be greater than the maximum possible value of $\gamma_{j,l}|\hat{g}_{k,j,l}|/\epsilon - \gamma_{j,l}$, for $l \in \{1, \ldots, L\}$. ■

References

[1] A. Shahmansoori, G. Seco-Granados, and H. Wymeersch, "Robust power allocation for OFDM wireless network localization," in *Proc. IEEE Int. Conf. Commun. Workshop (ICCW)*, London, U.K., Jun. 2015, pp. 718–723.

[2] A. H. Sayed, A. Tarighat, and N. Khajehnouri, "Network-based wireless location: Challenges faced in developing techniques for accurate wireless location information," *IEEE Signal Process. Mag.*, vol. 22, no. 4, pp. 24–40, Jul. 2005.

[3] H. Godrich, A. M. Haimovich, and R. S. Blum, "Target localization accuracy gain in MIMO radar-based systems," *IEEE Trans. Inf. Theory*, vol. 56, no. 6, pp. 2783–2803, Jul. 2005.

[4] F. Meshkati, H. V. Poor, and S. C. Schwartz, "Energy-efficient resource allocation in wireless networks," *IEEE Signal Process. Mag.*, vol. 24, no. 3, pp. 58–68, May 2007.

[5] Y. Shen, W. Dai, and M. Z. Win, "Power optimization for network localization," *IEEE/ACM Trans. Netw.*, vol. 22, no. 4, pp. 1337–1350, Aug. 2014.

[6] W. Dai, Y. Shen, and M. Z. Win, "Distributed power allocation for cooperative wireless network localization," *IEEE J. Sel. Areas Commun.*, vol. 33, no. 1, pp. 28–40, Jan. 2015.

[7] Y. Shen and M. Z. Win, "Fundamental limits of wideband localization—Part I: A general framework," *IEEE Trans. Inf. Theory*, vol. 56, no. 10, pp. 4956–4980, Oct. 2010.

[8] Y. Shen, H. Wymeersch, and M. Z. Win, "Fundamental limits of wideband localization—Part II: Cooperative networks," *IEEE Trans. Inf. Theory*, vol. 56, no. 10, pp. 4981–5000, Oct. 2010.

[9] W. W.-L. Li, Y. Shen, Y. J. Zhang, and M. Z. Win, "Robust power allocation for energy-efficient location-aware networks," *IEEE/ACM Trans. Netw.*, vol. 21, no. 6, pp. 1918–1930, Dec. 2013.

[10] J. A. Del Peral-Rosado, J. A. Lopez-Salcedo, G. Seco-Granados, F. Zanier, and M. Crisci, "Achievable localization accuracy of the positioning reference signal of 3GPP LTE," in *Proc. IEEE Int. Conf. Localization GNSS (ICL-GNSS)*, Starnberg, Germany, Jun. 2012, pp. 1–6.

[11] A. Mutapcic and S. Boyd, "Cutting-set methods for robust convex optimization with pessimizing oracles," *Optim. Methods Softw.*, vol. 24, no. 3, pp. 381–406, Jun. 2009. [Online]. Available: http://dx.doi.org/10.1080/10556780802712889

[12] M. D. Larsen, G. Seco-Granados, and A. L. Swindlehurst, "Pilot optimization for time-delay and channel estimation in OFDM systems," in *Proc. IEEE Int. Conf. Acoust., Speech Signal Process. (ICASSP)*, Prague, Czech Republic, May 2011, pp. 3564–3567.

[13] L. Sanguinetti and M. Morelli, "An initial ranging scheme for the IEEE 802.16 OFDMA uplink," *IEEE Trans. Wireless Commun.*, vol. 11, no. 9, pp. 3204–3215, Sep. 2012.

[14] M. Morelli, L. Sanguinetti, and H. V. Poor, "A robust ranging scheme for OFDMA-based networks," *IEEE Trans. Commun.*, vol. 57, no. 8, pp. 2441–2452, Aug. 2009.

[15] S. M. Kay, *Fundamentals of Statistical Processing: Estimation Theory*. New York, NY, USA: Prentice-Hall, 2010.

[16] S. Boyd and L. Vandenberghe, *Convex Optimization*. New York, NY, USA: Cambridge Univ. Press, 2004.

[17] *Evolved Universal Terrestrial Radio Access (E-UTRA); User Equipment (UE) Radio Transmission and Reception (3GPP TS 36.101 V9.18.0 Rel. 9)*, Eur. Telecommun. Standards Inst. (ETSI), Sophia Antipolis Cedex, France.

[18] J. A. Del Peral-Rosado, "Evaluation of the LTE positioning capabilities in realistic navigation channels," Ph.D. dissertation, Dept. Telecomunicació Enginyeria Sistemes, Univ. Autonoma Barcelona, Barcelona, Spain, 2014.

[19] M. Grant and S. Boyd. (Aug. 2010). *CVX: MATLAB Software for Disciplined Convex Programming, Version 1.21*. [Online]. Available: http://cvxr.com/cvx

[20] A. J. Kleywegt, A. Shapiro, and T. Homem-de-Mello, "The sample average approximation method for stochastic discrete optimization," *SIAM J. Optim.*, vol. 12, no. 2, pp. 479–502, 2001.

Arash Shahmansoori received the B.Sc. degree (Hons.) in bioelectric engineering from Tehran Polytechnic, Tehran, Iran, in 2010, and the M.Sc. degree in signal processing from the Norwegian University of Science and Technology, Trondheim, Norway, in 2012. He is currently pursuing the Ph.D. degree in joint communication and navigation techniques with the SPCOMNAV Group, Universitat Autònoma de Barcelona. His current research interests include 5G technologies for positioning and communications.

Gonzalo Seco-Granados (S'97-M'02-SM'08) received the Ph.D. degree in telecommunications engineering from the Universitat Politècnica de Catalunya, in 2000, and the MBA degree from IESE Business School, in 2002. From 2002 to 2005, he was a member of the European Space Agency, involved in the design of the Galileo System. Since 2006, he has been an Associate Professor with the Department of Telecommunications and Systems Engineering, Universitat Autònoma de Barcelona, Spain. He has been a principal investigator of over 25 research projects. In 2015, he was a Fulbright Visiting Professor with the University of California at Irvine, Irvine, CA, USA. His research interests include the design of signals and reception techniques for satellite and terrestrial localization systems, multi-antenna receivers, and positioning with 5G technologies. He was a recipient of the ICREA Academia Award.

Henk Wymeersch (S'01–M'05) received the Ph.D. degree in electrical engineering/applied sciences from Ghent University, Belgium, in 2005. He was a Post-Doctoral Researcher with the Laboratory for Information and Decision Systems, Massachusetts Institute of Technology, from 2005 to 2009. He is currently a Professor of communication systems with the Department of Signals and Systems, Chalmers University of Technology, Sweden. His current research interests include cooperative systems and intelligent transportation. He served as an Associate Editor of the IEEE COMMUNICATION LETTERS (2009–2013), the IEEE TRANSACTIONS ON WIRELESS COMMUNICATIONS (since 2013), and the IEEE TRANSACTIONS ON COMMUNICATIONS (since 2016).